Conjugate transfer of heat and mass in unsteady flow of a micropolar fluid with wall couple stress

Cite as: AIP Advances **5**, 127125 (2015); https://doi.org/10.1063/1.4938551
Submitted: 11 August 2015 • Accepted: 10 December 2015 • Published Online: 18 December 2015

Asma Khalid, Ilyas Khan, Arshad Khan, et al.

View Online Export Citation CrossMark

ARTICLES YOU MAY BE INTERESTED IN

Heat and mass transfer analysis of unsteady MHD nanofluid flow through a channel with moving porous walls and medium
AIP Advances **6**, 045222 (2016); https://doi.org/10.1063/1.4945440

Magneto-hydrodynamic flow and heat transfer of a hybrid nanofluid in a rotating system among two surfaces in the presence of thermal radiation and Joule heating
AIP Advances **9**, 025103 (2019); https://doi.org/10.1063/1.5086247

Boundary layer flow and heat transfer to Carreau fluid over a nonlinear stretching sheet
AIP Advances **5**, 107203 (2015); https://doi.org/10.1063/1.4932627

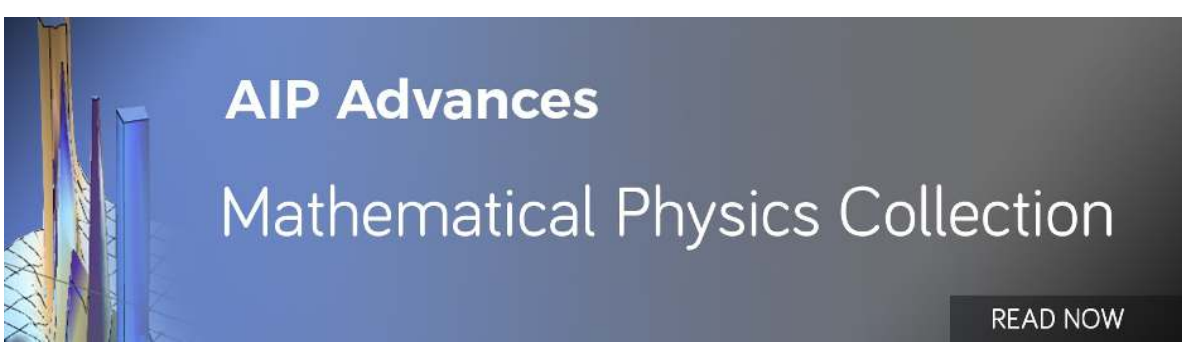

© 2015 Author(s).

AIP ADVANCES **5**, 127125 (2015)

Conjugate transfer of heat and mass in unsteady flow of a micropolar fluid with wall couple stress

Asma Khalid,[1,2] Ilyas Khan,[3] Arshad Khan,[2] and Sharidan Shafie[2]
[1]*Sardar Bahadur Khan Women's University, Brewery Road, 87300 Quetta, Pakistan*
[2]*Department of Mathematical Sciences, Faculty of Science, Universiti Teknologi Malaysia, 81310 UTM Skudai, Malaysia*
[3]*College of Engineering, Majmaah University, P.O. Box 66, Majmaah 11952, Saudi Arabia*

(Received 11 August 2015; accepted 10 December 2015; published online 18 December 2015)

This is an attempt to investigate the unsteady flow of a micropolar fluid with free convection caused due to temperature and concentration differences. Micropolar fluid is taken over a vertical plate oscillating in its own plane. Wall couple stress is engaged at the bounding plate together with isothermal temperature and constant mass diffusion. Problem is modelled in terms of coupled partial differential equations together with some physical conditions and then written in non-dimensional form. Exact solutions are determined using the Laplace transform method. For convenience, they are expressed in simplified form using exponential functions and complementary error functions. Using computational software MATHCAD, analytical results of velocity, temperature, microrotation and concentration are plotted in graphs and discussed for various embedded parameters. Results of skin friction, wall couple stress, rate of heat transfer (Nusselt number) and rate of mass transfer (Sherwood number) are also evaluated. Present results of micropolar fluid are graphically compared with published results of Newtonian fluid. It is found that micropolar fluid velocity is smaller than Newtonian fluid. © *2015 Author(s). All article content, except where otherwise noted, is licensed under a Creative Commons Attribution 3.0 Unported License.* [http://dx.doi.org/10.1063/1.4938551]

I. INTRODUCTION

Newtonian fluids problems described by Navier Stokes equations are simple and convenient. Because of this reason, they are extensively studied in the past few decades. However, in terms of applications Newtonian fluids are limited.[1–5] As there are many important fluids such as elastomers, certain oils, blood, clay coating, soap, greases, suspensions and many emulsions are quite important due to their industrial applications but unfortunately, we cannot use Navier Stokes equations to describe them. Main reason is the linear relation between stress and rate of strain for Newtonian fluids. This relation is nonlinear for above mentioned fluids. They are known as non-Newtonian fluids in the literature. Since non-Newtonian fluids play a significant role in industry as well as in various disciplines of engineering. In particular, some important applications are found in the fields of biorheology, geophysics, chemical and petroleum industries.[6–10]

Rheological characteristics of non-Newtonian fluids are described by their constitutive equations. Because of complex nature of non-Newtonian fluids, several models or constitutive equations have been suggested based on their empirical observations. Amongst them, one model was proposed by Eringen[11,12] using micromorphic fluid theory, known as micropolar fluids. Micropolar fluids poses microrotation and microinertia effects and constitute a significant branch of fluids. In literature micropolar fluids are used to describe flow characteristics of colloidal suspensions, geomor-phological sediments, liquid crystals, polymeric additives, haematological suspensions, lubricants and many other biological fluids.[13,14] Combined transfer of heat and mass in micropolar fluids plays an important role in chemical engineering, aerospace engineering and in industrial manufacturing process. Eringen and Lukaszewicz discussed fascinating characteristics of theory and applications of micropolor fluids.[15,16] Agarwal *et al.*[17] investigated heat transfer in micropolor

 ©Author(s) 2015.

fluid past a porous along a stationary wall. Ramachandran *et al.*[18] studied micropolar fluid in stagnation point flow. El-Arabawy[19] presented the micropolar fluid in the presence of radiation effects of suction/injection past a continuously moving plate. Nazar *et al.*[20] examined boundary layer flow of micropolar fluid past an isothermal sphere by taking the free convection. Cheng[21] discussed natural convection for micropolar fluids in combined transfer of heat and mass over a sphere accepting constant wall temperature together with constant wall concentration.

Sherief *et al.*[22] used the Laplace transform method and studied unsteady flow of a micropolar fluid from with suddenly moved plate. However, for inverse Laplace transform, they used complex inversion formula involving contour integration with several difficult and unsolved integrals. Aurangzaib *et al.*[23] considered the unsteady MHD mixed convection flow of micropolar fluid with heat and mass transfer over a vertical plate in a porous medium. Analysis of heat transfer from moving surfaces with internal heat generation in a micropolar fluid is carried out by El-Hakiem.[24] Hassanien *et al.*[25] investigated the natural convection boundary layer flow of a micropolar fluid. Ishak *et al.*[26] discussed the micropolar fluids with heat transfer over a stretching surface with variable heat flux whereas Lok *et al.*[27] reported the steady mixed convection flow near the stagnation point on a vertical surface of a micropolar fluid. Boundary layer stagnation point flow past a moving wall of a micropolar fluid by applying Runge-Kutta technique has been studied by Gorla.[28] Srinivasacharya and Rajyalakshmi[29] illustrated the problem of creeping flow of a micropolar fluid past a porous sphere. Abo-Eldahab and Ghonaim[30] presented the radiation effect on heat transfer of a micropolar fluid through a porous medium. Iyengar and Vani[31] examined the oscillatory flow in a micropolar fluid. Nadeem *et al.*[32] analyzed the MHD stagnation flow of a micropolar fluid through a porous medium. Analytic solution for heat and mass transfer problem of a micropolar fluid in a porous channel by using Differential Transformation Method (DTM) is carried out by Sheikholeslami *et al.*[33] The problem of fully developed natural convective micropolar fluid flow with slip condition in a vertical channel is presented by Ashmawy.[34] Damesh *et al.*[35] reported the micropolar fluid with unsteady natural convection heat transfer over a vertical surface with constant heat flux using numerical technique. Modatheri *et al.*[36] studied the oscillatory flow of a micropolar fluid over a vertical permeable plate in a porous medium with MHD effects. Devakar and Iyengar[37] discussed the Stokes' second problem for a micropolar fluid through by using state-space approach. Unsteady peristaltic flow of micropolar fluid in a finite channel is carried out by Pandey and Tripathi.[38] Javed *et al.*[39] gave the analytical solution for rotating flow of a micropolar fluid induced by a stretching surface. Mostafa *et al.*[40] illustrated the MHD flow and heat transfer of a micropolar fluid with slip velocity over a stretching surface with heat generation (absorption). Sajid *et al.*[41] analyzed the thin film flow of a micropolar fluid whereas Zia ul Haque *et al.*[42] examined the micropolar fluid behaviour on steady MHD free convection and mass transfer flow with constant heat and mass fluxes, joule heating and viscous dissipation. MHD micropolar fluid with unsteady free convection heat and mass transfer in the presence of thermo diffusion and thermal radiation is carried out by Olajuwon and Oahimire.[43] Abo-Dahab and Mohamed[44] reported the unsteady flow of rotating and chemically reacting MHD micropolar fluid in slip-flow regime with heat generation. Influence of heat with source or sink on MHD flow of micropolar fluids over a shrinking sheet with mass suction has been discussed by Sajjad and Farooq.[45] Mohanty *et al.*[46] numerically investigated heat and mass transfer effect of micropolar fluid over a stretching sheet using Runge–Kutta fourth order method with a shooting technique. Mishra *et al.*[47] studied MHD free convection flow of a micropolar fluid with heat source.

The aim of the present work is to provide exact solutions for the unsteady free convection flow of an incompressible micropolar fluid over an infinite vertical plate oscillating in its own plan. More exactly, the combined phenomenon of heat and mass transfer when the bounding plate takes wall couple stress with isothermal temperature and constant mass diffusion is studied. Mathematical formulation of the problem with exact solution is given in Section II. Section III presents the closed form solution in terms of exponential functions and complementary error functions, which are obtained by using Laplace transform technique.[48–51] Obtained solutions can be easily customized to obtain similar solutions for Newtonian fluids and many other simpler problems as shown in Section IV. Graphical results with detailed discussion are given in Section V followed by conclusion in Section VI.

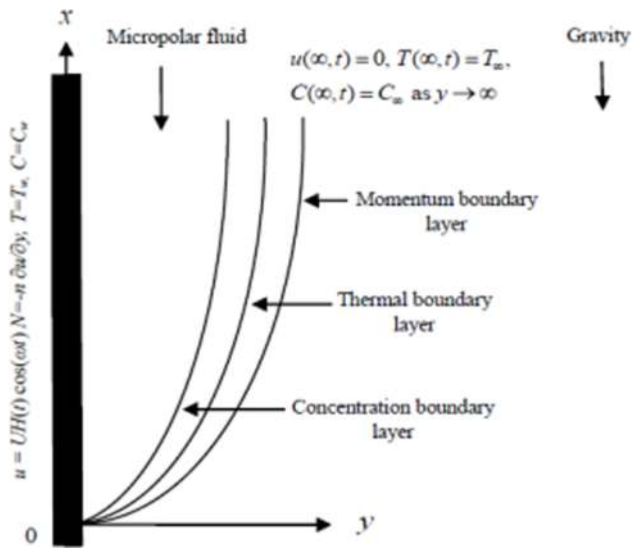

FIG. 1. Flow configuration.

II. MATHEMATICAL FORMULATION

Consider the unsteady boundary layer flow of an incompressible micropolar fluid in the region $y > 0$ driven by a plane surface located at $y = 0$ with a fixed end at $x = 0$. The physical configuration of the problem is shown in Figure 1.[47] It is assumed that at the initial moment $t = 0$, both the plate and the fluid are at rest at the constant temperature T_∞ and concentration C_∞. At time $t = 0^+$ the plate begins to oscillate in its plane ($y = 0$) according to

$$\boldsymbol{V} = UH(t)\cos(\omega t)\,\mathbf{i};\ \ t > 0, \tag{1}$$

where $H(t)$ is the unit step function, U is the amplitude of the motion, $\mathbf{i}$ is the unit vector in the vertical flow direction and ω is the frequency of oscillation of the plate. At the same time, the plate temperature and concentration level are raised to T_w and C_w which are thereafter maintained constants. Assume that the velocity, temperature and concentration are functions of y and t only.

Taking the usual Boussinesq's approximation, the unsteady flow is governed by the following set of partial differential equations:[40,45]

$$\rho\frac{\partial u}{\partial t} = (\mu+\alpha)\frac{\partial^2 u}{\partial y^2} + \rho g\beta_f(T - T_\infty) + \rho g\beta_c(C - C_\infty) + \alpha\frac{\partial N}{\partial y}, \tag{2}$$

$$\rho j\frac{\partial N}{\partial t} = \gamma_0\frac{\partial^2 N}{\partial y^2}, \tag{3}$$

$$\rho c_p\frac{\partial T}{\partial t} = k\frac{\partial^2 T}{\partial y^2}, \tag{4}$$

$$\frac{\partial C}{\partial t} = D\frac{\partial^2 C}{\partial y^2}. \tag{5}$$

The appropriate initial and boundary conditions are given as

$$u(y,0) = 0,\ N(y,0) = 0,\ T(y,0) = T_\infty,\ C(y,0) = C_\infty \text{ for all } y \ge 0, \tag{6}$$

$$u(0,t) = H(t)U\cos(\omega t),\ N(0,t) = -n\frac{\partial u}{\partial y}(0,t),\ T_\infty(0,t) = T_w \text{ and } C(0,t) = C_w,\ t > 0, \tag{7}$$

$$u(\infty,t) \to 0,\ \ N(\infty,t) \to 0,\ T(\infty,t) \to T_\infty \text{ and } C(\infty,t) \to C_\infty \text{ as } \ y \to \infty. \tag{8}$$

Here u is velocity, μ is dynamic viscosity, ρ is density, g is gravitational acceleration, α is vortex viscosity, t is time, T is the temperature, C is the species concentration, D is the mass diffusivity,

β_f is volumetric coefficient of thermal expansion, β_c is volumetric coefficient of expansion with concentration, N is the microrotation whose direction of rotation is in the xy-plane, j is microinertia per unit mass, γ_0 is spin gradient viscosity, c_p is heat capacity at constant pressure, k is thermal conductivity and ωt is phase angle. Three different values of $0 \leq n \leq 1$, when $n = 0$, which indicates $N = 0$ at the wall represents concentrated particle flows in which the microelements close to the wall surface are unable to rotate, this situation is also known as strong concentration of microelements. When $n = 1/2$, it indicates the vanishing of anti-symmetric part of the stress tensor and denotes weak concentration of microelements. The last case when $n = 1$ is used for the modelling of turbulent boundary layer flows.[44] The spin gradient viscosity γ_0, measures the relationship between the coefficients of viscosity and micro-inertia, is defined as

$$\gamma_0 = \left(\mu + \frac{\alpha}{2}\right) j\,.$$

To reduce the above equations (2)-(8) into their non-dimensional forms, we establish the following non-dimensional quantities,

$$y^* = \frac{U}{\nu} y,\ t^* = \frac{U^2}{\nu} t,\ u^* = \frac{u}{U},\ N^* = \frac{\nu}{U^2} N,\ \theta = \frac{T - T_\infty}{T_w - T_\infty},\ \phi = \frac{C - C_\infty}{C_w - C_\infty},\ \omega^* = \frac{\nu}{U^2}\omega,\ j^* = \frac{U^2}{\nu^2} j. \tag{9}$$

Implementing equation (9) into equations (2)-(5), we obtain the following non-dimensional partial differential equations (* symbol is omitted for simplicity)

$$\frac{\partial u}{\partial t} = (1+\beta)\frac{\partial^2 u}{\partial y^2} + \beta\frac{\partial N}{\partial y} + Gr\theta + Gm\phi, \tag{10}$$

$$\frac{\partial N}{\partial t} = \frac{1}{\eta}\frac{\partial^2 N}{\partial y^2}, \tag{11}$$

$$\Pr\frac{\partial \theta}{\partial t} = \frac{\partial^2 \theta}{\partial y^2}, \tag{12}$$

$$\frac{\partial \phi}{\partial t} = \frac{1}{Sc}\frac{\partial^2 \phi}{\partial y^2}. \tag{13}$$

The corresponding initial and boundary conditions take the following non-dimensional forms:

$$u(y,0) = 0,\ N(y,0) = 0,\ \theta(y,0) = 0,\ \phi(y,0) = 0 \ \text{for all}\ y \geq 0, \tag{14}$$

$$u(0,t) = H(t)\cos(\omega t),\ N(0,t) = -n\frac{\partial u}{\partial y}(0,t),\ \theta(0,t) = 1,\ \phi(0,t) = 1,\ t > 0, \tag{15}$$

$$u(\infty,t) \to 0,\ N(\infty,t) \to 0,\ \theta(\infty,t) \to 0,\ \phi(\infty,t) \to 0 \ as\ y \to \infty. \tag{16}$$

where

$$Gr = \frac{\nu g(T_w - T_\infty)\beta_T}{U^3},\ Gm = \frac{\nu g(C_w - C_\infty)\beta_c}{U^3},\ \beta = \frac{\alpha}{\mu},\ \Pr = \frac{\mu c_p}{k},\ \eta = \frac{\mu j}{\gamma_0},\ Sc = \frac{\nu}{D},$$

are the Grashof number, modified Grashof number, microrotation parameter, Prandtl number, dimensionless spin gradient and Schmidt number, respectively.

III. EXACT SOLUTIONS

Applying the Laplace transforms to equations (10)-(13), and using conditions (14-16), the following solutions in the transformed (y,q) plane

$$\begin{aligned}\bar{u}(y,q) &= a_4\frac{q}{(q^2+\omega^2)}e^{-y\sqrt{\beta_0 q}} + a_5\frac{q}{(q^2+\omega^2)}e^{-y\sqrt{\eta q}} + a_6\frac{1}{q^2}e^{-y\sqrt{\beta_0 q}} \\ &\quad + a_7\frac{1}{q^2}e^{-y\sqrt{\eta q}} - a_8\frac{1}{q^2}e^{-y\sqrt{\Pr q}} - a_9\frac{1}{q^2}e^{-y\sqrt{Scq}},\end{aligned} \tag{17}$$

$$\overline{N}(y,q) = \frac{a_1}{\sqrt{q}}e^{-y\sqrt{\eta q}} - \frac{a_1\omega}{2i}\frac{1}{\sqrt{q}(q+i\omega)}e^{-y\sqrt{\eta q}} + \frac{a_1\omega}{2i}\frac{1}{\sqrt{q}(q-i\omega)}e^{-y\sqrt{\eta q}} + \frac{a_2}{q\sqrt{q}}e^{-y\sqrt{\eta q}}, \tag{18}$$

$$\bar{\theta}(y,q) = \frac{1}{q}e^{-y\sqrt{q\mathrm{Pr}}}, \tag{19}$$

$$\bar{\phi}(y,q) = \frac{1}{q}e^{-y\sqrt{Scq}}. \tag{20}$$

By taking the inverse Laplace transforms of above equations, see (i), (ii), (iii) and (iv),

$$u(y,t) = u_1(y,t) + u_2(y,t) - u_3(y,t) - u_4(y,t) + u_5(y,t) + u_6(y,t) - u_7(y,t) - u_8(y,t). \tag{21}$$

$$N(y,t) = N_1(y,t) + N_2(y,t), \tag{22}$$

$$\theta(y,t) = \theta_1(y,t), \tag{23}$$

$$\phi(y,t) = \phi_1(y,t), \tag{24}$$

with

$$u_1(y,t) = \left(\frac{a_4}{4}\right)H(t)e^{-i\omega t}\left[e^{-y\sqrt{-i\omega\beta_0}}\mathrm{erfc}\left(\frac{y}{2}\sqrt{\frac{\beta_0}{t}} - \sqrt{-i\omega t}\right) + e^{y\sqrt{-i\omega\beta_0}}\mathrm{erfc}\left(\frac{y}{2}\sqrt{\frac{\beta_0}{t}} + \sqrt{-i\omega t}\right)\right],$$

$$u_2(y,t) = \left(\frac{a_4}{4}\right)H(t)e^{i\omega t}\left[e^{-y\sqrt{i\omega\beta_0}}\mathrm{erfc}\left(\frac{y}{2}\sqrt{\frac{\beta_0}{t}} - \sqrt{i\omega t}\right) + e^{y\sqrt{i\omega\beta_0}}\mathrm{erfc}\left(\frac{y}{2}\sqrt{\frac{\beta_0}{t}} + \sqrt{i\omega t}\right)\right],$$

$$u_3(y,t) = \left(\frac{a_5}{4}\right)H(t)e^{-i\omega t}\left[e^{-y\sqrt{-i\omega\eta}}\mathrm{erfc}\left(\frac{y}{2}\sqrt{\frac{\eta}{t}} - \sqrt{-i\omega t}\right) + e^{y\sqrt{-i\omega\eta}}\mathrm{erfc}\left(\frac{y}{2}\sqrt{\frac{\eta}{t}} + \sqrt{-i\omega t}\right)\right],$$

$$u_4(y,t) = \left(\frac{a_5}{4}\right)H(t)e^{i\omega t}\left[e^{-y\sqrt{i\omega\eta}}\mathrm{erfc}\left(\frac{y}{2}\sqrt{\frac{\eta}{t}} - \sqrt{i\omega t}\right) + e^{y\sqrt{i\omega\eta}}\mathrm{erfc}\left(\frac{y}{2}\sqrt{\frac{\eta}{t}} + \sqrt{i\omega t}\right)\right],$$

$$u_5(y,t) = a_6\left[\left(t + \frac{y^2\beta_0}{2}\right)\mathrm{erfc}\left(\frac{y}{2}\sqrt{\frac{\beta_0}{t}}\right) - y\sqrt{\beta_0}\sqrt{\frac{t}{\pi}}e^{-\frac{y^2\beta_0}{4t}}\right],$$

$$u_6(y,t) = a_7\left[\left(t + \frac{y^2\eta}{2}\right)\mathrm{erfc}\left(\frac{y}{2}\sqrt{\frac{\eta}{t}}\right) - y\sqrt{\eta}\sqrt{\frac{t}{\pi}}e^{-\frac{y^2\eta}{4t}}\right],$$

$$u_7(y,t) = a_8\left[\left(t + \frac{y^2\mathrm{Pr}}{2}\right)\mathrm{erfc}\left(\frac{y}{2}\sqrt{\frac{\mathrm{Pr}}{t}}\right) - y\sqrt{\mathrm{Pr}}\sqrt{\frac{t}{\pi}}e^{-\frac{y^2\mathrm{Pr}}{4t}}\right],$$

$$u_8(y,t) = a_9\left[\left(t + \frac{y^2Sc}{2}\right)\mathrm{erfc}\left(\frac{y}{2}\sqrt{\frac{Sc}{t}}\right) - y\sqrt{Sc}\sqrt{\frac{t}{\pi}}e^{-\frac{y^2Sc}{4t}}\right],$$

$$N_1(y,t) = a_1\left[\frac{1}{\sqrt{\pi t}}e^{-\frac{y^2\eta}{4t}}\right] - a_3\left[\frac{1}{2\sqrt{i\omega}}e^{i\omega t}\left[e^{-y\sqrt{i\omega\eta}}\mathrm{erfc}\left(\frac{y}{2}\sqrt{\frac{\eta}{t}} - \sqrt{i\omega t}\right) - e^{y\sqrt{i\omega\eta}}\mathrm{erfc}\left(\frac{y}{2}\sqrt{\frac{\eta}{t}} + \sqrt{i\omega t}\right)\right]\right]$$

$$N_2(y,t) = a_3\left[\frac{1}{2\sqrt{-i\omega}}e^{-i\omega t}\left[e^{-y\sqrt{-i\omega\eta}}\mathrm{erfc}\left(\frac{y}{2}\sqrt{\frac{\eta}{t}} - \sqrt{-i\omega t}\right) - e^{y\sqrt{-i\omega\eta}}\mathrm{erfc}\left(\frac{y}{2}\sqrt{\frac{\eta}{t}} + \sqrt{-i\omega t}\right)\right]\right] + a_2\left[2\sqrt{\frac{t}{\pi}}e^{-\frac{y^2\eta}{4t}} - y\sqrt{\eta}\,\mathrm{erfc}\left(\frac{y}{2}\sqrt{\frac{\eta}{t}}\right)\right],$$

$$\theta_1(y,t) = \mathrm{erfc}\left(\frac{y}{2}\sqrt{\frac{\mathrm{Pr}}{t}}\right),$$

$$\phi_1(y,t) = \mathrm{erfc}\left(\frac{y}{2}\sqrt{\frac{Sc}{t}}\right),$$

where

$$a_1 = \frac{\left(n\sqrt{\beta_0}\right)(\eta-\beta_0)}{\left(\eta-\beta_0+n\beta\beta_0\sqrt{\eta\beta_0}-n\beta_0\beta\eta\right)},$$

$$a_2 = A_1 nGr\sqrt{\beta_0}\frac{(\eta-\beta_0)}{\left(\eta-\beta_0+n\beta\beta_0\sqrt{\eta\beta_0}-n\beta_0\beta\eta\right)} + A_2 nGm\sqrt{\beta_0}\frac{(\eta-\beta_0)}{\left(\eta-\beta_0+n\beta\beta_0\sqrt{\eta\beta_0}-n\beta_0\beta\eta\right)}$$
$$-A_1 nGr\sqrt{\Pr}\frac{(\eta-\beta_0)}{\left(\eta-\beta_0+n\beta\beta_0\sqrt{\eta\beta_0}-n\beta_0\beta\eta\right)} - A_2 nGm\sqrt{Sc}\frac{(\eta-\beta_0)}{\left(\eta-\beta_0+n\beta\beta_0\sqrt{\eta\beta_0}-n\beta_0\beta\eta\right)},$$

$$a_3 = \frac{a_1\omega}{2i},\quad a_4 = 1-A_0a_1,\quad a_5 = A_0a_1,\quad a_6 = GrA_1+GmA_2-a_2A_0,$$
$$a_7 = a_2A_0,\quad a_8 = GrA_1,\quad a_9 = GmA_2,\ \beta_0 = \frac{1}{1+\beta}$$
$$A_0 = \frac{\beta\beta_0\sqrt{\eta}}{\eta-\beta_0},\ \ A_1 = \frac{\beta_0}{\Pr-\beta_0},\ \ A_2 = \frac{\beta_0}{Sc-\beta_0}.$$

It is obvious from the solutions of velocity and microrotation given by equations (21) and (22), are valid for $\Pr \neq \beta_0$, and $Sc \neq \beta_0$. The corresponding solutions for $\Pr = \beta_0$, and $Sc = \beta_0$, can be easily obtained by substituting $\Pr = Sc = \beta_0$ into equations (12) and (13), and follow a similar procedure as discussed above.

The skin friction co-efficient at the wall is

$$\tau = -\left(1+\frac{1}{\alpha}\right)\frac{\partial u}{\partial y}\,|_{y=0} + \alpha N|_{y=0},$$

and dimensionless form obtained as

$$C_f = \frac{2\tau_w^*}{\rho U^2} = 2\left[1+(1-n)+\beta\right]u'(0)\,. \tag{25}$$

Similarly, the dimensionless couple wall stress co-efficient at the plate is expressed as:

$$C_m = \gamma_0\frac{\partial N}{\partial y}\bigg|_{y=0},$$

and in dimensionless form,

$$C_m^* = \frac{C_m}{\mu jU} = (1+\beta)\,N'(0)\,. \tag{26}$$

The Nusselt number and Sherwood number can be calculated as:

$$Nu = x\frac{(\partial T/\partial y^*)\,y^*}{T_\infty - T_w} = 0,$$

$$NuRe_x^{-1} = -\theta'(0)\,, \tag{27}$$

$$Sh = x\frac{(\partial C/\partial y^*)\,y^*}{C_\infty - C_w} = 0,$$

$$ShRe_x^{-1} = -\phi'(0)\,, \tag{28}$$

where $Re_x = \frac{\upsilon x}{U}$ is the local Reynolds number.

IV. PARTICULAR CASES

A. Stokes first problem

By taking the phase angle $\omega t = 0$, which correspond the impulsive motion of the plate, then equation (21) and (22) yields

$$u(y,t) = u_5(y,t) + u_6(y,t) - u_7(y,t) - u_8(y,t) + u_9(y,t) - u_{10}(y,t)\,, \tag{29}$$
$$N(y,t) = N_3(y,t), \tag{30}$$

where

$$u_9(y,t) = a_4 H(t)\left[\operatorname{erfc}\left(\frac{y}{2}\sqrt{\frac{\beta_0}{t}}\right)\right],$$

$$u_{10}(y,t) = a_5 H(t)\left[\operatorname{erfc}\left(\frac{y}{2}\sqrt{\frac{\eta}{t}}\right)\right],$$

$$N_3(y,t) = a_1\left[\frac{1}{\sqrt{\pi t}}e^{-\frac{y^2\eta}{4t}}\right] + a_2\left[2\sqrt{\frac{t}{\pi}}e^{-\frac{y^2\eta}{4t}} - y\sqrt{\eta}\operatorname{erfc}\left(\frac{y}{2}\sqrt{\frac{\eta}{t}}\right)\right].$$

B. Without thermal and mass concentration effects

In the absence of free convection, which numerically corresponds to $Gr = 0$ and $Gm = 0$, the relevant result for velocity is obtained as:

$$u(y,t) = u_1(y,t) + u_2(y,t) - u_3(y,t) - u_4(y,t). \tag{31}$$

C. In case of Newtonian fluid

In the absence of microrotation parameter, which is numerically corresponds to $\beta = 0$, alternatively $\beta_0 = 1$, the solution for velocity reduce to the corresponding solution for Newtonian fluid.

$$u_N(y,t) = u_1'(y,t) + u_2'(y,t) + u_5'(y,t) - u_7(y,t) - u_8(y,t), \tag{32}$$

where

$$u_1'(y,t) = \left(\frac{a_4}{4}\right)H(t)e^{-i\omega t}\left[e^{-y\sqrt{-i\omega}}\operatorname{erfc}\left(\frac{y}{2}\sqrt{\frac{1}{t}} - \sqrt{-i\omega t}\right) + e^{y\sqrt{-i\omega}}\operatorname{erfc}\left(\frac{y}{2}\sqrt{\frac{1}{t}} + \sqrt{-i\omega t}\right)\right],$$

$$u_2'(y,t) = \left(\frac{a_4}{4}\right)H(t)e^{i\omega t}\left[e^{-y\sqrt{i\omega}}\operatorname{erfc}\left(\frac{y}{2}\sqrt{\frac{1}{t}} - \sqrt{i\omega t}\right) + e^{y\sqrt{i\omega}}\operatorname{erfc}\left(\frac{y}{2}\sqrt{\frac{1}{t}} + \sqrt{i\omega t}\right)\right],$$

$$u_5'(y,t) = a_6\left[\left(t + \frac{y^2}{2}\right)\operatorname{erfc}\left(\frac{y}{2}\sqrt{\frac{1}{t}}\right) - y\sqrt{\frac{t}{\pi}}e^{-\frac{y^2}{4t}}\right].$$

V. GRAPHICAL RESULTS AND DISCUSSION

In this section final results are computed for different physical parameters which are presented by mean of graphs. Parameter of physical interest are microrotation parameter β, dimensionless

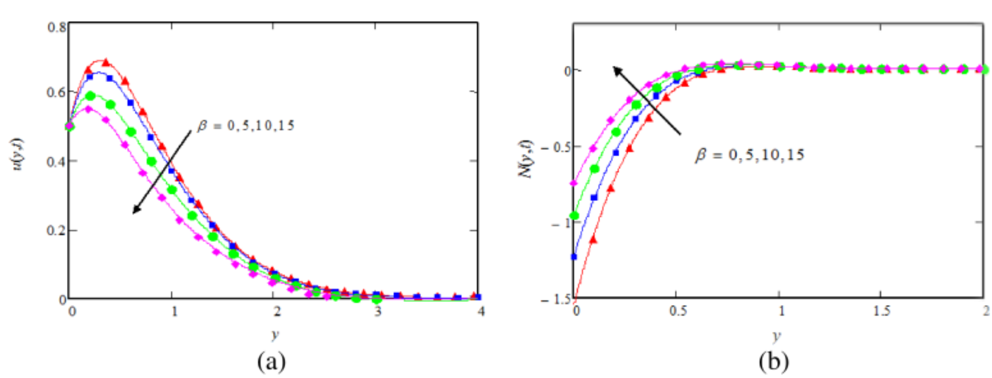

FIG. 2. (a) Velocity profiles for different values of β, when $\Pr = 0.3, \eta = 1.5, n = 0.6, Gr = Gm = 5, Sc = 0.2$, $\omega t = \frac{\pi}{3}$ and $t = 0.6$; (b) Microrotations for different values of β, when $\Pr = 0.3, \eta = 1.5, n = 0.6, Gr = Gm = 5, Sc = 0.2$, $\omega t = \frac{\pi}{3}$ and $t = 0.6$.

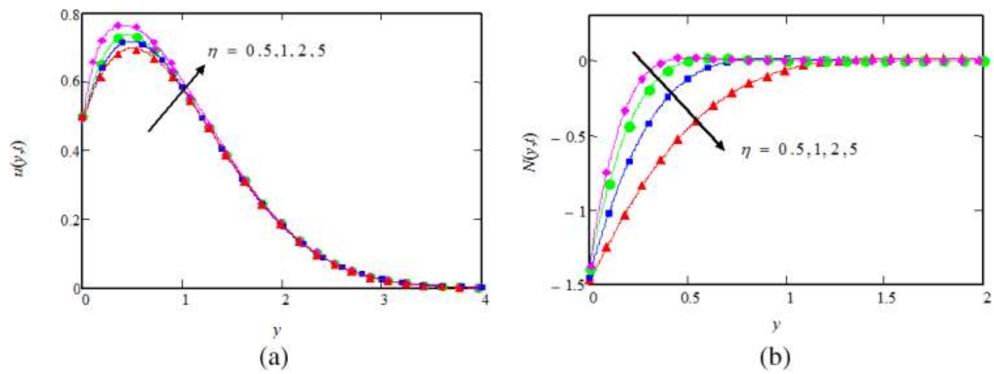

FIG. 3. (a) velocity profiles for different values of η, when $\mathrm{Pr}=0.3, \eta=1.5, n=0.6, Gr=Gm=5, Sc=0.2, \omega t=\frac{\pi}{3}$ and $t=0.6$; (b) Microrotations for different values of η, when $\mathrm{Pr}=0.3, \eta=1.5, n=0.6, Gr=Gm=5, Sc=0.2, \omega t=\frac{\pi}{3}$ and $t=0.6$.

spin gradient viscosity parameter η, microelement n, Prandtl number Pr, Grashof number Gr, modified Grashof number Gm, Schmidt number Sc, phase angle ωt and time t. Note that the direction of the arrow shows the increasing values of the involved parameter.

Influence of microrotation parameter β on velocity $u(y,t)$ and the microrotation $N(y,t)$ is depicted in Figures 2(a) and 2(b). These graphs show that velocity decreases whereas microrotation increases with increasing β. Obviously, velocity satisfies the imposed boundary conditions in equations (15) and (16). It is clear that the velocity is greater for a Newtonian fluid ($\beta=0$) with the flow as compared with micropolar fluids until its peak value reaches. On the other hand, the microrotation $N(y,t)$ takes the negative values of the gradient of velocity at the plate surface and approaching to zero as one move away from the plate surface as shown in Figure 2(b). This fact totally aggresses with imposed conditions on microrotation (see equations (15) and (16)). The influence of microrotation parameter β on velocity $u(y,t)$ and microrotation $N(y,t)$ is identical with published results of Abo-Dahab and Mohamed.[44] The effect of spin gradient viscosity parameter η on the velocity and microrotation is plotted in Figures 3(a) and 3(b). It is observed that velocity increases with increasing η, while reverse effect is observed for microrotation.

Figures 4(a) and 4(b) depict the effects of parameter n, which relates to the microgyration vector and the shear stress on the linear velocity and the microrotation profiles. It is found that velocity increases with increasing values of n, whereas the magnitude of the microrotation increases with an increase of n close to the plate but decreases with increasing distance from the plate. It can be further seen from Figure 4(a) that variation in the thickness of the momentum boundary layer due to the microgyration vector is smaller. From microrotation condition in equation (15), we can

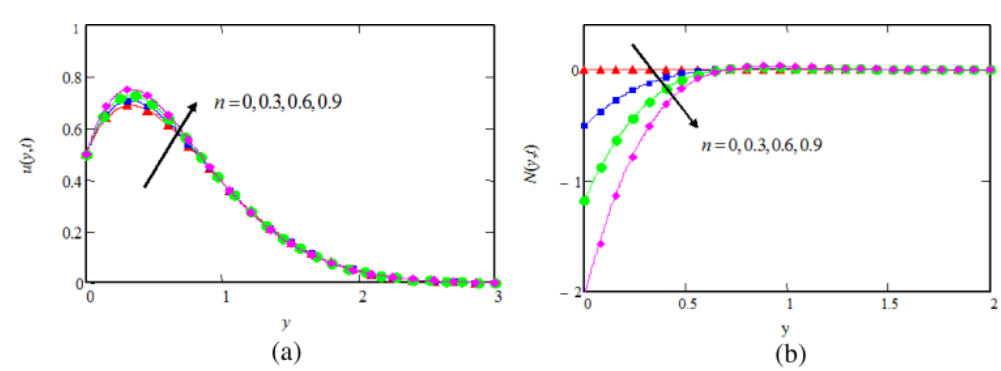

FIG. 4. (a) Velocity profiles for different values of n, when $\mathrm{Pr}=0.3, \beta=0.5, \eta=1.5, Gr=5, Gm=10, Sc=2$, $\omega t=\frac{\pi}{3}$ and $t=0.2$; (b) Microroations for different values of n, when $\mathrm{Pr}=0.3, \beta=0.5, \eta=1.5, Gr=5, Gm=10, Sc=2$, $\omega t=\frac{\pi}{3}$ and $t=0.2$.

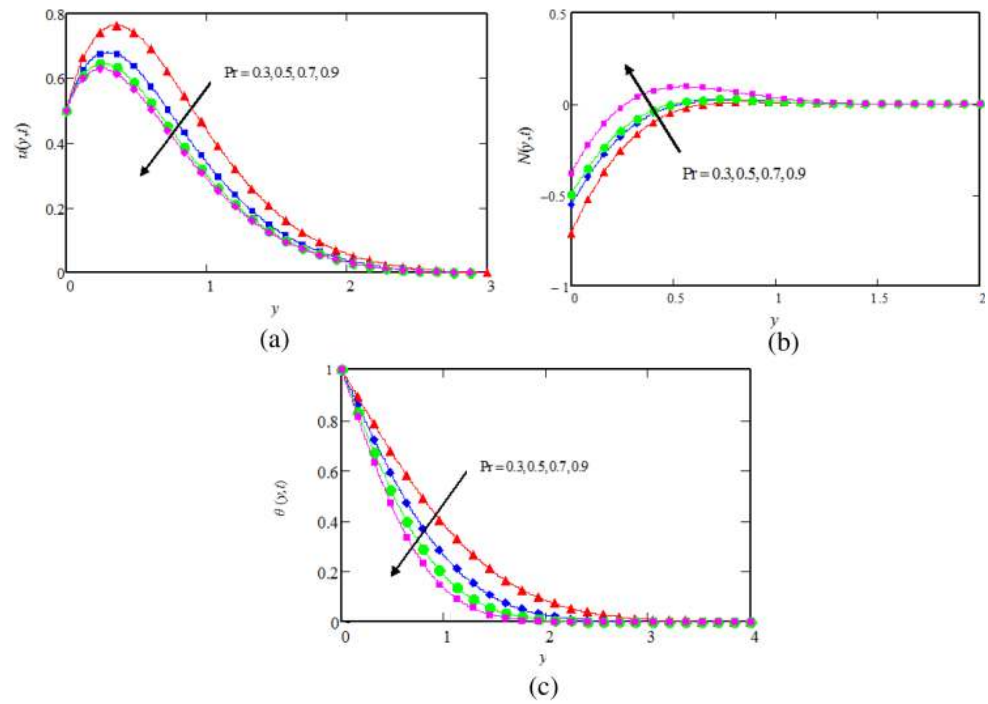

FIG. 5. (a) Velocity profiles for different values of Pr, when $\beta = 0.5, \eta = 1.5, n = 0.6, Gr = Gm = 5, Sc = 0.2$, $\omega t = \frac{\pi}{3}$ and $t = 0.6$; (b) Microrotations for different values of Pr, when $\beta = 0.5, \eta = 1.5, n = 0.6, Gr = Gm = 5, Sc = 0.2$, $\omega t = \frac{\pi}{3}$ and $t = 0.6$; (c) Temperature profiles for different values of Pr, when $t = 0.6$.

see that when $n = 0, N(y,t) = 0$ for all values of y greater than or equal to zero. This fact is shown in Figure 4(b). Figures 5(a), 5(b) and 5(c) present plots for velocity, microrotation, and temperature for different values of Prandtl number Pr. These graphs show that the influence of increasing values of Pr result in decreasing of the velocity, magnitude of the microrotation, and temperature as well. It is also true physically because, smaller values of Pr increase the thermal conductivity of the fluid and consequently heat is able to diffuse away more rapidly for higher values of Pr from the heated surface. This in the case of smaller Prandtl numbers, the rate of heat transfer is reduced and thermal boundary layer becomes thicker and rate of heat transfer is reduced. Figures 6(a) and 6(b) show variations in velocity and microrotation profiles for various values of Grashof number Gr. It is observed that an increase in Gr leads to an increase in velocity due to enhancement in the buoyancy

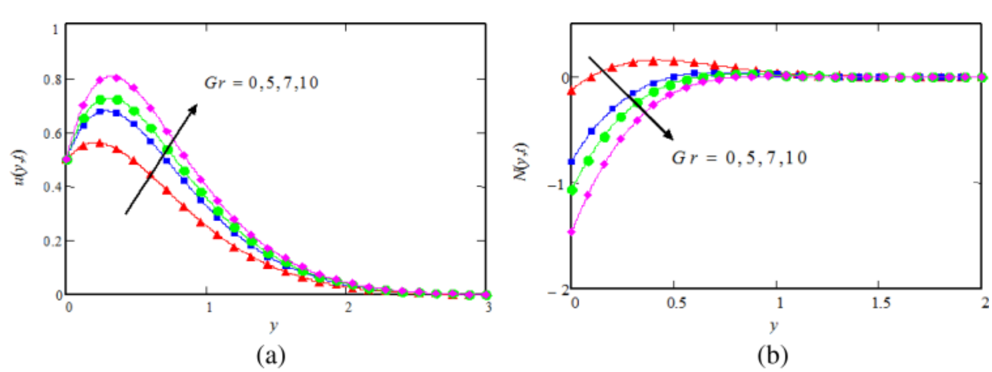

FIG. 6. (a) Velocity profiles for different values of Gr, when $\Pr = 0.3, \beta = 0.5, \eta = 1.5, n = 0.6, Gm = 5, Sc = 2$, $\omega t = \frac{\pi}{3}$ and $t = 0.2$; (b) Microrotaions for different values of Gr, when $\Pr = 0.3, \beta = 0.5, \eta = 1.5, n = 0.6, Gm = 5, Sc = 2$, $\omega t = \frac{\pi}{3}$ and $t = 0.2$.

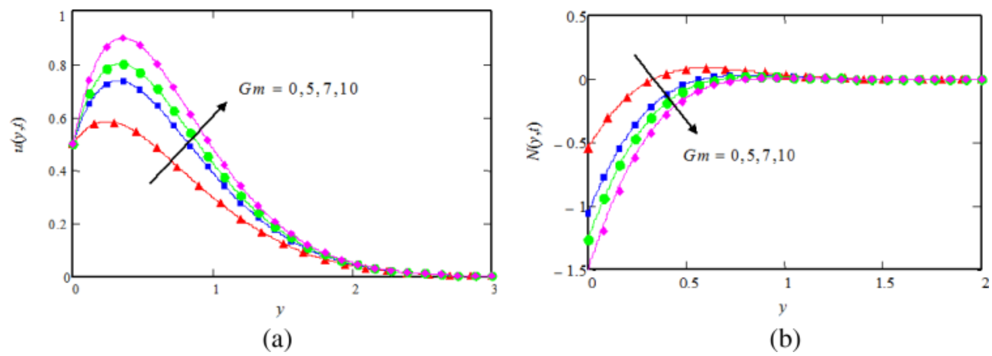

FIG. 7. (a) Velocity profiles for different values of Gm, when $\Pr = 0.3, \beta = 0.5, \eta = 1.5, n = 0.6, Gr = 5, Sc = 2$, $\omega t = \frac{\pi}{3}$ and $t = 0.2$; (b) Microroations for different values of Gm, when $\Pr = 0.3, \beta = 0.5, \eta = 1.5, n = 0.6, Gr = 5, Sc = 2$, $\omega t = \frac{\pi}{3}$ and $t = 0.2$.

force. Besides that magnitude of microrotation decreases for large values of Gr. For positive values of Gr correspond to cooling of the surface by natural convection whereas $Gr = 0$ shows the absence of heat transfer due to free convection. On the other hand, the plots of velocity and microrotation for different Gm, are presented in Figures 7(a) and 7(b). We noted that velocity distribution attains a maximum value in the neighborhood of the plate because of an increase in the buoyancy force due to concentration gradient and then decreases accurately to approach a free stream value. The curve corresponding to $Gm = 0$ represents the absence of free convection due to mass transfer. More exactly, the curves corresponding to $Gr = Gm = 0$ specifies, that the buoyancy force arising due to gradients of heat and mass transfers is absent.

Aim of Figures 8(a), 8(b) and 8(c) is to show the influence of Schmidt number Sc, on velocity, microrotation, and concentration profiles respectively. It is found from these figures, that with

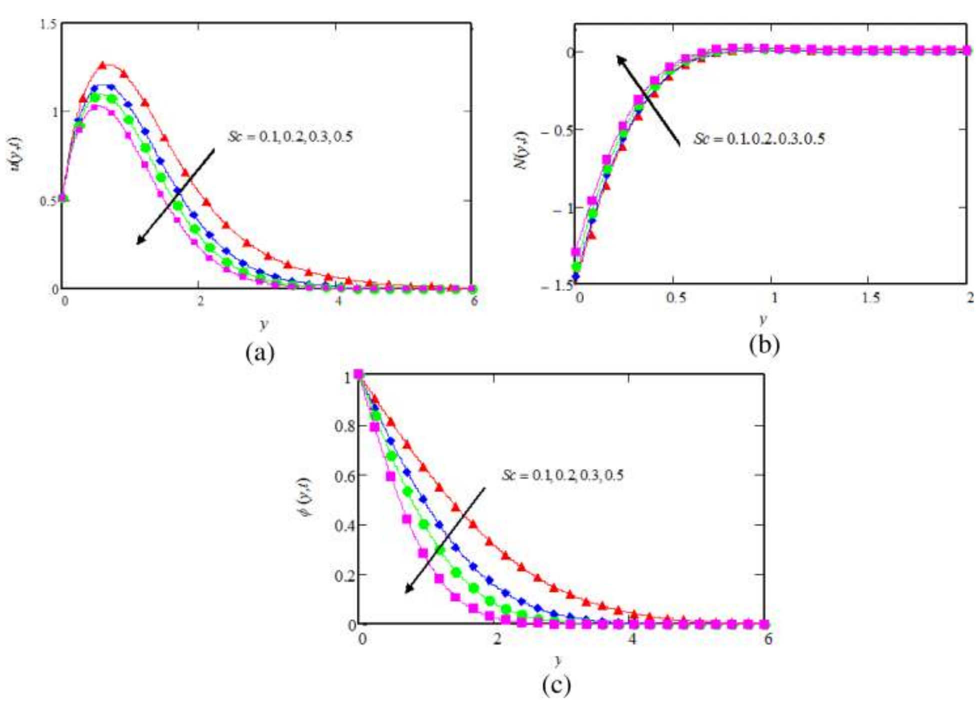

FIG. 8. (a) Velocity profiles for different values of Sc, when $\Pr = 0.3, \beta = 0.5, \eta = 1.5, Gr = 5, Gm = 10, n = 0.6$, $\omega t = \frac{\pi}{3}$ and $t = 0.2$; (b) Microrotations for different values of Sc, when $\Pr = 0.3, \beta = 0.5, \eta = 1.5, Gr = 5, Gm = 10, n = 0.6$, $\omega t = \frac{\pi}{3}$ and $t = 0.2$; (c) Concentration profiles for different values of Sc, when $\Pr = 0.3$.

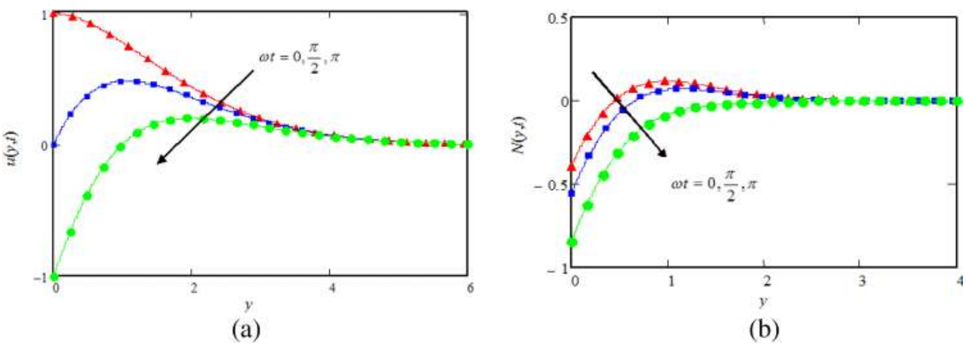

FIG. 9. (a) Velocity profiles for different values of ωt, when $\Pr = 0.3, \beta = 0.5, \eta = 1.5, Gr = 5, Gm = 10, n = 0.6$, $Sc = 1$ and $t = 0.2$; (b) Microrotaions for different values of ωt, when $\Pr = 0.3, \beta = 0.5, \eta = 1.5, Gr = 5, Gm = 10, n = 0.6$, $Sc = 1$ and $t = 0.2$.

increasing Sc, velocity is tending to decrease across the boundary layer. Besides that Figure 8(b) shows that the magnitude of microrotation decreases as Sc increases. Figure 8(c) depicts that an increase in Sc leads to a decrease in concentration profile. This figure reveals that an increase in Sc leads to a decrease in the concentration distribution, because the smaller values of Sc are equivalent to an increase in the chemical molecular diffusivity. In Figures 9(a) and 9(b) graphs are sketched for velocity and microtation profiles $u(y,t)$ and $N(y,t)$ for four different values of phase angle ωt. It is found that the velocity presents an oscillatory behaviour. Instead, the magnitude of microtation shows an increasing behaviour. Figure 9(a) reveals that velocity satisfies the imposed boundary condition (15). This figure can easily help us to check the accuracy of our results. Both velocity and microrotation have maximum values near the plate and decreasing with increasing distance from the plate and approaches zero as $y \to \infty$.

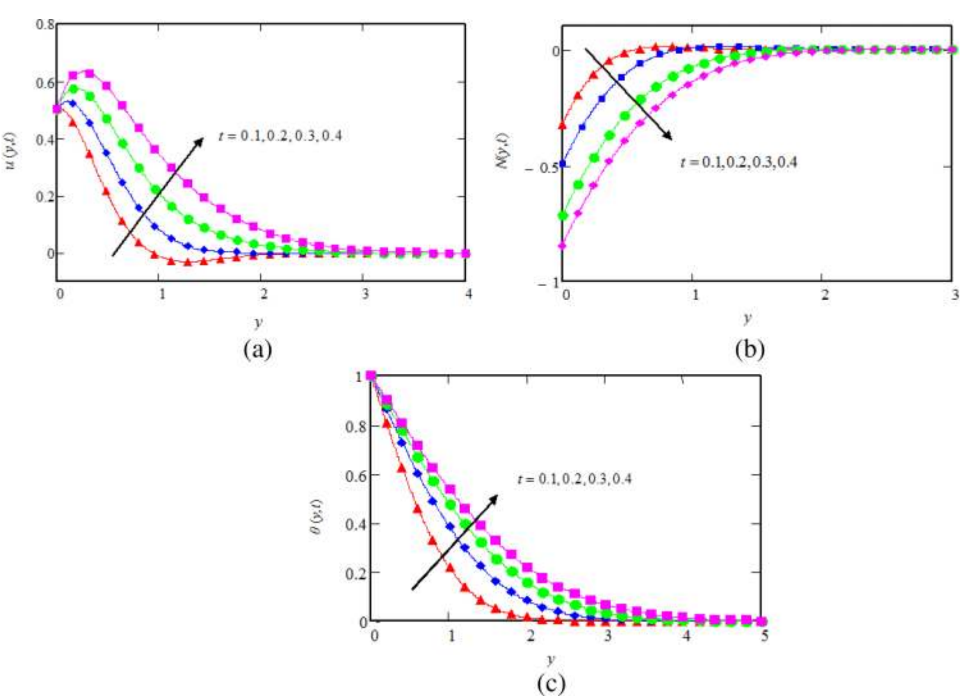

FIG. 10. (a) Velocity profiles for different values of t, when $\Pr = 0.3, \beta = 0.5, \eta = 1.5, Gr = 5, Gm = 10, n = 0.6$, $Sc = 1$ and $\omega t = \frac{\pi}{3}$; (b) Microroations for different values of t, when $\Pr = 0.3, \beta = 0.5, \eta = 1.5, Gr = 5, Gm = 10, n = 0.6$, $Sc = 1$ and $\omega t = \frac{\pi}{3}$; (c) Temperature profiles for different values of t, when $\Pr = 0.3$.

Figures 10(a), 10(b) and 10(c) exhibit the effects of time t on velocity, microrotation and temperature profiles. It is seen that velocity and microtation have opposite relation with increasing values of t, whereas temperature increases with increasing t. Figure 11 is sketched in order to show the comparison of micropolar fluid velocity given by equation (21) with Newtonian fluid velocity given by equation (32). It is obvious from this figure that the boundary layer thickness of micropolar fluid velocity is smaller than the boundary layer thickness of Newtonian fluid. More exactly, velocity is smaller for micropolar fluid compare to Newtonian fluid. In this comparison graph, we found that our results are identical to those reported in (Ref. 40, see Figure 10).

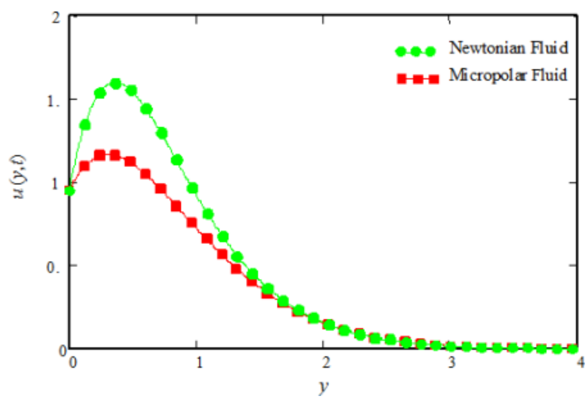

FIG. 11. Comparison of micropolar fluid velocity (when $\beta = 1$), with Newtonian fluid velocity (when $\beta = 0$) and $\omega t = \frac{\pi}{3}$.

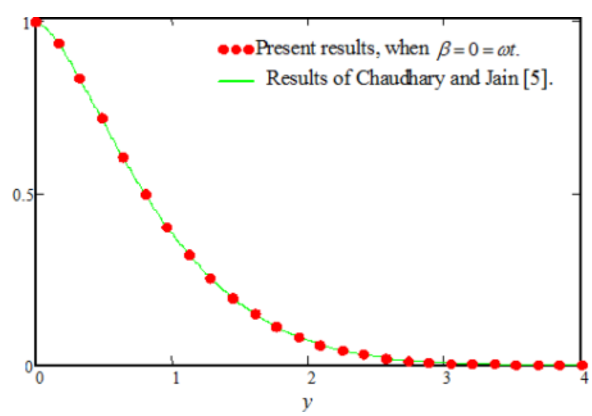

FIG. 12. Comparison of the present results (when $\beta = 0$), with results obtained by Chaudhary and Jain,[5] see Equation (19), when $t = 0.2$, $\omega t = 0$ and $M = \frac{1}{K} = 0$.

TABLE I. Numerical results for skin friction.

β	n	Pr	Gr	Gm	Sc	ωt	t	τ
0.5	0.6	0.3	5	5	0.2	$\pi/4$	0.6	3.2386
2	0.6	0.3	5	5	0.2	$\pi/4$	0.6	3.3057
0.5	**0.9**	0.3	5	5	0.2	$\pi/4$	0.6	2.5837
0.5	0.6	**0.7**	5	5	0.2	$\pi/4$	0.6	3.4454
0.5	0.6	0.3	**7**	5	0.2	$\pi/4$	0.6	2.9142
0.5	0.6	0.3	5	**7**	0.2	$\pi/4$	0.6	2.6354
0.5	0.6	0.3	5	5	**0.5**	$\pi/4$	0.6	3.5012
0.5	0.6	0.3	5	5	0.2	$\pi/2$	0.6	3.4441
0.5	0.6	0.3	5	5	0.2	$\pi/4$	**0.9**	2.9097

TABLE II. Numerical results for wall couple stress.

β	n	Pr	Gr	Gm	Sc	ωt	t	τ
0.5	0.6	0.3	5	5	0.2	$\pi/4$	0.6	2.1322
2	0.6	0.3	5	5	0.2	$\pi/4$	0.6	1.9754
0.5	**0.9**	0.3	5	5	0.2	$\pi/4$	0.6	1.4587
0.5	0.6	**0.7**	5	5	0.2	$\pi/4$	0.6	1.6312
0.5	0.6	0.3	**7**	5	0.2	$\pi/4$	0.6	0.7485
0.5	0.6	0.3	5	**7**	0.2	$\pi/4$	0.6	1.3651
0.5	0.6	0.3	5	5	**0.5**	$\pi/4$	0.6	2.0392
0.5	0.6	0.3	5	5	0.2	$\pi/2$	0.6	1.9929
0.5	0.6	0.3	5	5	0.2	$\pi/4$	**0.9**	1.0834

In order to check the accuracy of present results, the velocity profiles of present result, equation (21) is compared with existing results in literature Chaudhary and Jain.[5] This comparison is shown in Figure 12. Excellent agreement is found. Numerical results for skin friction and wall couple stress are shown in table I and table II, respectively.

VI. CONCLUDING REMARKS

In this work a combined phenomenon of heat and mass transfer in the unsteady flow of an incompressible, homogeneous micropolar fluid past an oscillating vertical plate with isothermal temperate and constant mass diffusion has been investigated. The governing equations of the flow, together with initial and boundary conditions were written in the non-dimensional forms. By means of the Laplace transform technique the closed forms solutions for the velocity, microrotation, temperature, and concentration have expressed in terms of exponential and complementary error functions. Based on the obtained solutions and using some graphical illustrations generated with the MATHCAD software, the following main points are concluded.

- Velocity across the boundary layer increases with increasing η, n, Gr, Gm and t whereas decreases with increasing values of β, Pr, Sc and ωt.
- Magnitude of microrotation on the plate is decreases with increasing η, n, Gr, Gm and t, while increases with increasing β, Pr, Sc and ωt.
- Temperature increases with increasing t, whereas concentration decreases with increasing Sc.
- The velocity is smaller for micropolar fluids than for Newtonian fluids.
- Solution (21) is found in excellent agreement with those obtain by Chaudhary and Jain.[5]

APPENDIX

$$\text{(i)}\quad L^{-1}\left\{\frac{1}{q^2}e^{-y\sqrt{q}}\right\} = \left[\left(t+\frac{y^2}{2}\right)\operatorname{erfc}\left(\frac{y}{2\sqrt{t}}\right) - y\sqrt{\frac{t}{\pi}}e^{-\frac{y^2}{4t}}\right],$$

$$\text{(ii)}\quad L^{-1}\left\{\frac{1}{q\sqrt{q}}e^{-y\sqrt{q}}\right\} = \left[2\sqrt{\frac{t}{\pi}}e^{-\frac{y^2}{4t}} - y\operatorname{erfc}\left(\frac{y}{2\sqrt{t}}\right)\right],$$

$$\text{(iii)}\quad L^{-1}\left\{\frac{1}{q+c}e^{-y\sqrt{q}}\right\} = \frac{e^{-ct}}{2}\left[e^{-y\sqrt{-c}}\operatorname{erfc}\left(\frac{y}{2\sqrt{t}} - \sqrt{-ct}\right) + e^{y\sqrt{-c}}\left(\operatorname{erfc}\frac{y}{2\sqrt{t}} + \sqrt{-ct}\right)\right],$$

$$\text{(iv)}\quad L^{-1}\left\{\frac{1}{\sqrt{q}(q-c)}e^{-y\sqrt{q}}\right\} = \frac{e^{-ct}}{2\sqrt{c}}\left[e^{-y\sqrt{-c}}\operatorname{erfc}\left(\frac{y}{2\sqrt{t}} - \sqrt{-ct}\right) - e^{y\sqrt{-c}}\left(\operatorname{erfc}\frac{y}{2\sqrt{t}} + \sqrt{ct}\right)\right].$$

[1] M. Sajid, I. Pop, and T. Hayat, "Fully developed mixed convection flow of a visco-elastic fluid between permeable parallel vertical plates," Computational Mathematics with Applications **59**, 493-488 (2010).

[2] M. I. Anwar, I. Khan, S. Shafie, and M. Z. Salleh, "Conjugate effects of heat and mass transfer of nano fluids over a non-linear stretching sheet," International Journal of Physical Sciences **7**, 4081-4092 (2012).

[3] M. E. Erdogan, "A note on the unsteady flow of a viscous fluid due to an oscillating plane wall," International Journal of Nonlinear Mechanics **35**, 1–6 (2000).
[4] R. S. Tripathy, G. C. Dash, S. R. Mishra, and S. Baag, "Chemical reaction effect on MHD free convective surface over a moving vertical plane through porous medium," Alexandria Engineering Journal **54**(3), 673-679 (2015).
[5] R. C. Chaudhary and A. Jain, "Combined heat and mass transfer effects on MHD free convection flow past an oscillating plate embedded in porous medium," Romania Journal of Physics **52**, 505–524 Bucharest (2007).
[6] M. Erdogan, "On unsteady motions of a second-order fluid over a plane wall," International Journal of Non-Linear Mechanics **38**, 1045–1051 (2003).
[7] C. Fetecau, C. Fetecau, and J. Zierep, "Decay of a potential vortex and propagation of a heat wave in a second grade fluid," International Journal of non-Linear Mechanics **37**, 1051–1056 (2002).
[8] C. Fetecau and C. Fetecau, "Starting solutions for some unsteady unidirectional flows of a second grade fluid," International Journal of Engineering Science **43**, 781–789 (2005).
[9] W.A. Khan and A. Aziz, "Natural convection flow of a nanofluid over a vertical plate with uniform surface heat flux," International Journal of Thermal Sciences **50**(7), 1207–1214 (2011).
[10] C. Fetecau, Corina Fetecau, and M. Rana, "General solutions for the unsteady flow of second-grade fluids over an infinite plate that applies arbitrary shear to the fluid," Zeitschrift für Naturforschung A. A Journal of Physical Sciences **66**, 753-759 (2011).
[11] A. C. Eringen, "Theory of Micropolar Fluids," Journal of Mathematics and Mechanics **16**, 1-18 (1966).
[12] A. C. Eringen, "Theory of Thermomicropolar Fluids," Journal of Mathematical Analysis and Applications **38**, 480-496 (1972).
[13] T. Ariman, M. A. Turk, and N. D. Sylvester, "Microcontinuum Fluid Mechanics -A Review," International journal of Engineering Science **11**, 905-930 (1973).
[14] T. Ariman, M. A. Turk, and N. D. Sylvester, "Applications of microcontinuum fluid mechanics review," International journal of Engineering Science **12**, 273-293 (1974).
[15] A. C. Eringen, *Microcontinuum Field Theories II: Fluent Media* (Springer, New York, 2001).
[16] G. Lukaszewicz, *Micropolar Fluids: Theory and Applications* (Birkhauser, Basel, 1999).
[17] R. S. Agarwal and C. Dhanapal, "Flow and heat transfer in a micropolar fluid past a flat plate with suction and heat sources," International Journal Engineering Science **26**, 1257-1266 (1988).
[18] P. S. Ramachandran and M. N. Mathur, "Heat transfer in boundary layer flow of a micropolar fluid past a curved surface with suction and injection," International Journal Engineering Science **17**, 625-639 (1979).
[19] H. A. M. El-Arabawy, "Effect of suction/injection on the flow of a micropolar fluid past a continuously moving plate in the presence of radiation," International Journal Heat Mass Transfer **46**, 1471–1477 (2003).
[20] R. Nazar *et al.*, "Free convection boundary layer on an isothermal sphere in a micropolar fluid," International Communications in Heat and Mass Transfer **29**, 377-386 (2002).
[21] C. Y. Cheng, "Natural convection heat and mass transfer from a sphere in micropolar fluids with constant wall temperature and concentration," International Communications, Heat and Mass Transfer **35**, 750-755 (2008).
[22] H. H. Sherief, M. S. Faltas, and E. A. Ashmawy, "Exact solution for the unsteady flow of a semi-infinite micropolar fluid," Acta Mechanica Sinica **27**, 354-359 (2011).
[23] Aurangzaib, A. R. M. Kasim, N. F. Mohammad, and S. Sharidan, "Unsteady MHD mixed convection flow with heat and mass transfer over a vertical plate in a micropolar fluid-saturated porous medium," Journal of Applied Science and Engineering **16**, 141-150 (2013).
[24] M. A. El-Hakiem, "Heat transfer from moving surfaces in a micropolar fluid with internal heat generation," Journal of Engineering and Applied Sciences **1**, 30-36 (2014).
[25] I. A. Hassanien, A. J. Bakier, and R. S. R. Gorla, "Natural convection boundary layer flow of a micropolar fluid," Zeitschrift für Angewandte Mathematik und Mechanik **77**, 751-755 (1997).
[26] A. Ishak, R. Nazar, and I. Pop, "Heat transfer over a stretching surface with variable heat flux in micropolar fluids," Physics Letters A **372**, 559–561 (2008).
[27] Y. Y. Lok, N. Amin, D. Campean, and I. Pop, "Steady mixed convection flow of a micropolar fluid near the stagnation point on a vertical surface," International Journal Numerical Methods Heat Fluid Flow **15**, 654–670 (2005).
[28] R. S. R. Gorla, "Micropolar boundary layer flow at stagnation on a moving wall," International Journal of Engineering Science **21**, 25-33 (1983).
[29] D. Srinivasacharya and I. Rajyalakshmi, "Creeping flow of a micropolar fluid past a porous sphere," Applied Mathematics and Computation **153**, 843–854 (2004).
[30] E. M. Abo-Eldahab and A. F. Ghonaim, "Radiation effect on heat transfer of a micropolar fluid through a porous medium," Applied Mathematics and Computation **169**, 500–510 (2005).
[31] K. Vafai and C. L. Tien, "Boundary and inertia effects on flow and heat transfer in porous media," International Journal Heat Mass Transfer **24**, 195-203 (1981).
[32] S. Nadeem, M. Hussain, and M. Naz, "MHD stagnation flow of a micropolar fluid through a porous medium," Meccanica **45**, 869-880 (2010).
[33] M. Sheikholeslami1, H. R. Ashorynejad1, D. D. Ganji1, and M. M. Rashidi, "Heat and mass transfer of a micropolar fluid in a porous channel," Communications in Numerical Analysis **2014**, 1-20 (2014).
[34] E.A. Ashmawy, "Fully developed natural convective micropolar fluid flow in a vertical channel with slip," Journal of the Egyptian Mathematical Society (2014), http://dx.doi.org/10.1016/j.joems.2014.06.019.
[35] R. A. Damesh, T. A. Al-Azab, B. A. Shannak, and M. A. Husein, "Unsteady natural convection heat transfer of micropolar fluid over a vertical surface with constant heat flux," Turkish Journal of Engineering and Environmental Sciences **31**, 225-233 (2007).
[36] M. Modatheri, A. M. Rashadi, and A. J. Chamkha, "An analytical study of MHD heat and mass transfer oscillatory flow of a micropolar fluid over a vertical permeable plate in a porous medium," Turkish Journal of Engineering Environmental Science **33**, 245–25 (2009).

[37] M. Devakar1 and T. K. V. Iyengar, "Stokes' second problem for a micropolar fluid through state-space approach," Energy Conversion and Management **52**, 934–945 (2011).
[38] S. K. Pandey and D. Tripathi, "Unsteady peristaltic flow of micro-polar fluid in a finite channel," Z. Naturforsch **66a**, 181–192 (2011).
[39] T. Javed, I. Ahmad, Z. Abbas, and T. Hayat, "Rotating flow of a micropolar fluid induced by a stretching surface," Z. Naturforsch **65a**, 829–836 (2010).
[40] A. A. Mostafa, E. Shimaa Mahmoud, and Waheed, "MHD flow and heat transfer of a micropolar fluid over a stretching surface with heat generation (absorption) and slip velocity," Journal of the Egyptian Mathematical Society **20**, 20–27 (2012).
[41] M. Sajid, N. Ali, and T. Hayat, "On exact solutions for thin film flows of a micropolar fluid," Communications in nonlinear science and numerical simulation **14**, 451–461 (2009).
[42] Md. Zia ul Haque, Md. Mahmud Alam, M. Ferdows, and A. Postelnicu, "Micropolar fluid behaviors on steady MHD free convection and mass transfer flow with constant heat and mass fluxes, joule heating and viscous dissipation," Journal of King Saud University – Engineering Sciences **24**, 71–84 (2012).
[43] B.I. Olajuwon and J.I. Oahimire, "Unsteady free convection heat and mass transfer in an MHD micropolar fluid in the presence of thermo diffusion and thermal radiation," International Journal of Pure and Applied Mathematics **84**, 15-37 (2013).
[44] S. M. Abo-Dahab and R. A. Mohamed, "Unsteady flow of rotating and chemically reacting MHD micropolar fluid in slip-flow regime with heat generation," International Journal of Thermophysics **34**, 2183-2208 (2013).
[45] H. Sajjad and A. Farooq, "Effects of heat source/sink on MHD flow of micropolar fluids over a shrinking sheet with mass suction," Journal of Basic and Applied Scientific Research **4**, 207-215 (2014).
[46] B. Mohanty, S. R. Mishra, and H. B. Pattnaik, "Numerical investigation on heat and mass transfer effect of micropolar fluid over a stretching sheet," Alexandria Engineering Journal **54**(2), 223-232 (2015).
[47] S. R. Mishra, G.C. Dash, and P. K. Pattnaik, "Flow of heat and mass transfer on MHD free convection in a micropolar fluid with heat source," Alexandria Engineering Journal **54**(3), (2015).
[48] P. Puri and P.K. Kythe, "Some inverse Laplace transforms of exponential form," ZAMP Journal of Applied Mathematics and Physics **39**, 150–156 (1988).
[49] L. Debnath and D. Bhatta, *Integral transforms and their applications* (Chapman & Hall/CRC Press, Boca Raton, FL, 2007).
[50] M. Narahari and L. Debnath, "Some new convolution properties and inversion formulas of Laplace transforms," Integral Transforms and Special Functions **25**, 412-422 (2014).
[51] C. J. Toki and J.N. Tokis, "Exact solutions for the unsteady free convection flows on a porous plate with time-dependent heating," ZAMM Journal of Applied Mathematics and Mechanics **87**, 4-13 (2007).